LINKS BETWEEN MICROSEISMS AND EXTREME WAVES DURING TYPHOONS

Li-Ching Lin[1], Jing-Yih Liou[2], Hwung-Hweng Hwung[3], Frédéric Bouchette[4], Samuel Meulé[5]

Ocean-Solid Earth coupling is the main forcing of generating seismic noise. It has been well known that seismic noise in the frequency band from 0.05 to about 1 Hz results from ocean waves. Components of noise spectrum, also called microseisms, are used to study extreme waves during typhoons. During the KUN–SHEN project (2011-2014), wave measurements have collected at the Cigu coast of Taiwan and compared with microseisms observations at inland seismometers from Broadband Array in Taiwan for Seismology (BATS) network. By comparing between background and storm induced microseisms, peaks in the noise spectrum can be divided in to two frequency bands. Comparison of microseism band between 0.1 and 0.2 Hz with buoys in the deep sea shows a strong correlation of seismic amplitude with storm generating waves, implying that this energy portion could originates at the remote regions. Microseism amplitudes above 0.2 Hz show a good correlation with wind-generating waves near coasts. Findings also show that maximum amplitudes of two different portions have the significant time lag, implying that source locations of generating microseisms can be identified. Results indicate that secondary microseisms observed at inland sites can be a potential tool of tracking typhoon motions and monitoring extreme waves near coasts in real time. Seismic noise in the 1-10Hz band has rough correlation with wave activities in swash zone. Further examination is required to investigate those differences.

Keywords: microseisms; extreme waves; typhoons

INTRODUCTION

Microseisms are continuous ground oscillations recorded at seismometers and wildly introduced for decades since Wiechert (1904). Observations usually show that two peaks dominate the seismic spectrum in the frequency band between 0.04 and 1Hz are nearly linked to wave periods between 5 and 25 second. Lower amplitude peaks at 0.04-0.1 Hz as primary microseism and larger one at 0.1-1 Hz as secondary microseism (Haubrick et al. 1963; Haubrich and McCamy, 1969). Microseism generations have been explained by Longuet-Higgins (1950) for secondary microseisms and Hasselmann (1963) for primary microseisms.

Generation mechanisms are commonly based on the nonlinear wave-wave interaction to excite pressure pulse into the seafloor. Secondary microseisms are generated when progressive waves interact in opposite directions. The resulting pressure fluctuation into the seafloor yields the continuous ground oscillation at the double frequency (DF) of ocean waves of the same frequency. In terms of the theory, the depth of water is responsible for the efficiency of microseism generation in the resonance effect. For that reason, amplitudes of secondary microseisms can be amplified in certain water depths. Comparisons between measured and modeled ground displacements of the secondary microseism have been quantitatively tested by applying Longuet-Higgins' idea in deep waters of the North Atlantic Ocean (Keder et al. 2008). In addition, primary microseisms are only generated in the shallow waters by the similar process. Typically the secondary spectral peak is much larger than the primary peak (Haubrich and McCamy, 1969). More details on observations and generations of microseisms are discussed by Ebeling et al. (2012).

Thus wind-driven waves under interference conditions play important role on DF microseisms in any water depths. For a growth and movement of distant typhoon, the amplitude of DF microseisms varies with the intensity of typhoons while the generating waves in opposing directions interact around the depression region. For a typhoon approaches to coasts, interference occurs when incident waves reflected from an irregular shoreline and then the amplitude of DF microseisms is generated in the middle between a typhoon and shoreline (Cooper and Longuet-Higgins, 1951). Recent studies indicate that spectra of recoding DF microseisms at both inland and seafloor sites may be composed of two frequency bands originated from local and remote forcings (Bromirski et al. 2005; Stephen et al. 2003). Total of ocean microseisms may be the sum contribution from several regions in which wave-wave interaction occurs (Kedar et al. 2008; Tabulevich et al. 1976). In fact, the source regions are not likely

[1] International Wave Dynamics Research Center, National Cheng Kung University, Taiwan. Email: plih@gate.sinica.edu.tw
[2] Tainan Hydraulics Laboratory, National Cheng Kung University, Taiwan. Email: jyliou@mail.ncku.edu.tw
[3] Department of Hydraulic and Ocean Engineering, National Cheng Kung University, Taiwan. Email: hhhwung@mail.ncku.edu.tw
[4] GLADYS / OSU OREME, CNRS/ Université de Montpellier II, France. Email: frederic.bouchette@gmail.com
[5] CEREGE, Université Aix-Marseille, France. Email: meule@cerege.fr

to be identified by correlations of microseisms with ocean wave heights at a given site, which often suggests different levels of their coherence.

In order to understand the characteristics of DF microseisms associated with different source regions, we aim to analyze and investigate the spectra of DF microseisms and its link to western Pacific typhoons. The simple spectrum method proposed by Rabinovich (1997) is used to identify the source of wave induced microseisms associated with typhoons. This method is well applied to separate the external forcing of tsunamis from local resonances without any numerical and complex computations(Vich and Monserrat, 2009)

In this paper, we will examine source characteristics of secondary (DF) microseisms by inland seismometers during typhoons developed in the deep ocean and moved to shoreline in the shallow seas. In addition, the frequency above 0.1 Hz is discussed its correlation with sediment transport in the swash zone. Although this portion in such high frequency band is not well reported, the similar features may follow the seismic variations associated bedload particles transport in the river with high discharge conditions (Hsu et al. 2011; Schmandt et al. 2013).

DATA AND METHOD

Typhoons strike Taiwan coasts each year during summer season and some uncommon typhoons moving from South China Sea to Taiwan Strait could result in a significant impact in the south-western shoreline. Maximum wave heights exceed 6 m were recorded at Cigu waters (Fig. 1) in 2009-2012. In that period, ocean waves are recorded by the Cigu buoy at 18 m water depth. Wave observations are available from Central Weather Bureau (CWB), Taiwan. During the KUN–SHEN project (2011-2014), waves in shallow waters have been collected by ADCP sensors at 4 m and 7 m of water depth near the Cigu shoreline. In the typhoon seasons, the dominant source of microseisms was identified using the simple spectrum method (Rabinovich 1977) from continuous monitoring broadband seismometers at the Broadband Array in Taiwan for Seismology (BATS) network (Kao et al. 1998; available at http://bats.earth.sinica.edu.tw/). For this study, seismic data sampled at 20 Hz in horizontal and vertical instruments. In order to study characteristics of seismic noise during typhoons, the three most extreme waves were selected for examination the relationship between microseisms and ocean waves.

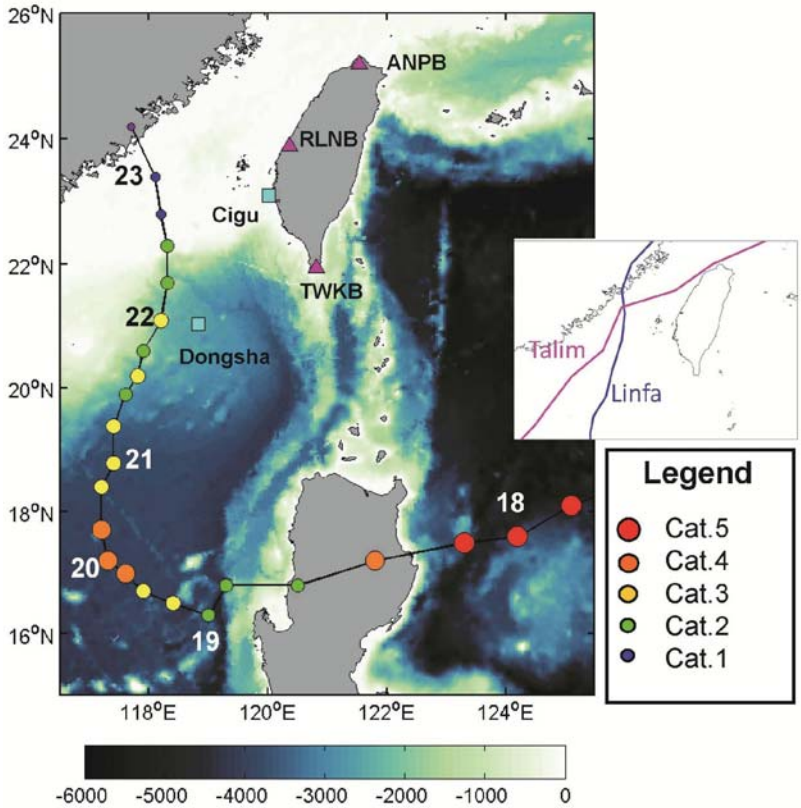

Figure 1. Locations of CWB buoys (squares) and inland seismic sites of BATS network (triangles). Detail track (line) and intensity (circles) of Typhoon Megi, 2010 is illustrated in each time step. The inset shows

tracks of two other typhoons around Taiwan Strait. Typhoon Lina of 2009 is at the category 1 cyclone; Typhoon Talim of 2012 at the level of tropical storm.

To reduce the earthquake influence in seismic noise, magnitudes that exceeded one standard deviations of each hour were to be eliminated in that time span. The spectrum method is applied to study the evolution of typhoon generated microseisms. This method is briefly outlined that observed seismic spectrum ($S_{obs}(\omega)$) during typhoons could be considered as the sum of the energy associated with the typhoon source ($S_r(\omega)$) and background activity ($S_b(\omega)$)

$$S_{obs}(\omega) = S_r(\omega) + S_{obs}(\omega) \tag{1}$$

If we may assume the topographic effect ($W(\omega)$) in any conditions, it can be considered as the same response in the spectral domain of the typhoon source and background activity.

$$S_r(\omega) = W(\omega)E_r(\omega),\ S_b(\omega) = W(\omega)E_b(\omega) \tag{2}$$

where $E_r(\omega)$ and $E_b(\omega)$ represent the external forcing during typhoon and background conditions respectively.

The spectral ratio for the typhoon source can be estimated from Eq (1) and Eq (2)

$$S_{obs}(\omega) / S_b(\omega) = \left[E_r(\omega) / E_b(\omega)\right] + 1 \tag{3}$$

which may present the source energy content during typhoons and the ratio is independent of the instrument location and entirely determined by the external forcing. Thus the spectral ratio is expected to have the similar response for typhoons at seismic sites.This method is used to correlate with the source of microseisms and waves throughout the oceans and along coastlines during typhoons.

OBSERVATIONS AND ANALYSIS

1. SEISMIC NOISE AT THE FREQUENCY BAND OF 0.1-1 Hz

Typhoon Megi of 2010 was recorded at the BTAS network in Taiwan (Fig. 1). This typhoon was chosen because it moved from South China Sea and the extreme wave height of 6.6 m was recorded at the Cigu buoy when the intensity of typhoon was at a category 2 cyclone. During this period, significant seismic changes in vertical velocity were found when the typhoon approached to Taiwan (Fig. 2). In the velocity waveforms, two energetic amplitude changes were identified when the typhoon initialed at Western Pacific Ocean along it track to South China Sea in the first time step and it developed again from South China Sea to Taiwan Strait in the following step. In addition, the time travel of the maximum amplitude varied with locations from south to north could suggest that observed typhoon-induced seismic noise could be associated with its moving close to each station.

By comparing typhoon-induced seismic noise with nearby wave heights observed by buoys, changes of seismic noise associated with waves in the second time step only supports the mechanism of wave generated microseisms during Typhoon Megi. In the first time step of this typhoon, no other strong correlation between both was found. Apparently it may generate by the wave-wave interaction in the typhoon radius.

In order to separate the different source from microseisms, RLNB seismic site was selected to demonstrate the spectral ratio of correlating with the source characteristics and waves for typhoon events. RLNB is about 20 km north of the Cigu coast. The hourly spectrum of vertical velocity was processed by the Fourier Fast Transform method with the hamming window for typhoons. In addition, the background has been averaged from the 10 calm days of 2010 when earthquake activities are also insignificant in Taiwan.

Figure 3 shows that dominant features at the frequency band of 0.05 and 1 Hz which is mainly affected by Typhoon Megi. In Figure 3a the seismic levels show two microseism peaks in the 0.05–0.15 Hz and 0.15-1Hz bands corresponding to primary and secondary microseisms respectively. With the increasing amplitude as typhoon approaching to Dongsha Island on October 22, peak of secondary microseisms is shifting to the frequency near 0.2 Hz. After the typhoon has passed and moved to Taiwan Strait, frequencies of the secondary microseism increase from 0.2 Hz to 0.4Hz.

For the spectral ratio at RLNB shown in Figure 3b, the topographic effect has removed to highlight the source of microseisms. The seismic levels concentrate at the frequency band between 0.1 and 0.2 Hz approximately and that dominant energy is well correlated the development of Typhoon Megi during two time steps described above. For that correlation, this part of secondary microseism is

most likely associated with the typhoon activity either in the remote area or at local seas. And the absence of dominant energy in the 0.1-0.2 Hz band could result from the undoubted wave-wave interaction as the intensity of the typhoon is reduced during the landfall in Philippines.

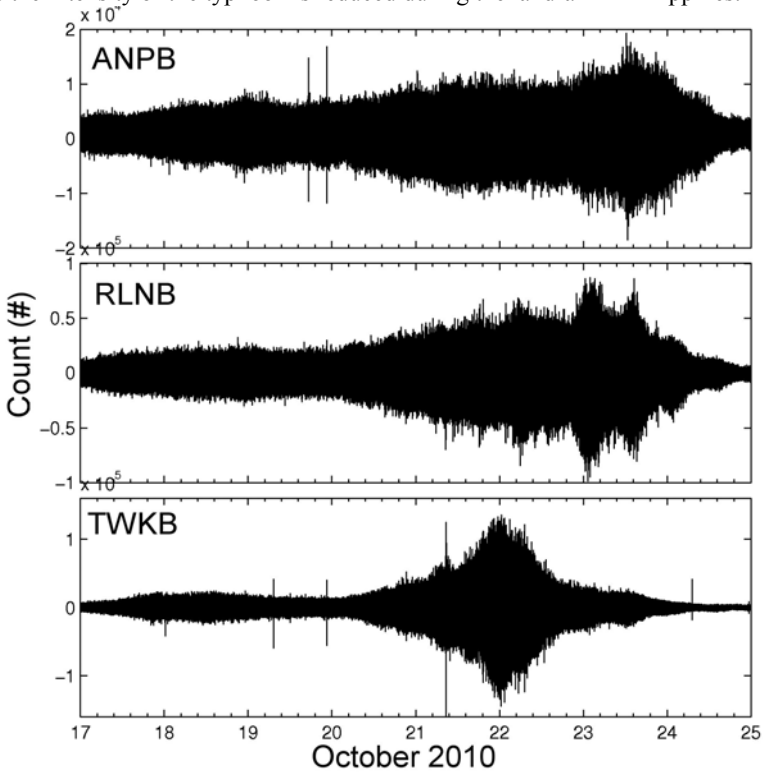

Figure 2. Vertical velocity records during Typhoon Megi from north (ANPB) to south (TWKB). Spike-like signals represent the earthquakes. Vertical scale shows the count records of seismometers.

Moreover, the most of such spectral ratio is affected locally by the wave height of 13 m (Fig. 3c) observed at the Dongsha buoy when the typhoon is closest to the station. Although the satellite derived wind speeds show no significant increasing on October 22, the buoy observation provides the strong evidence that microseisms of 0.1-0.2 Hz band is likely from the opposing waves for secondary microseism generation near Dongsha Island in South China Sea. Therefore, the pattern of spectral ratio suggests a common source at the frequency band of 0.1-0.2 Hz during the typhoon event. Detail analysis of typhoon source from Ocean Bottom Seismometers (OBS) will be separated to another paper to discuss the coherence of typhoon source and localization of source area.

Considering the swell propagation from the typhoon to the Cigu coast on October 22-23, that spectral ratio at the frequency above 0.2 Hz is more likely attributed to wave activities observed at the Cigu buoy shown in Figure 3c. Swell reflected from the south-western shoreline may primarily explain the source of generating secondary microseism at higher frequency (> 0.2Hz) in the shallow waters when typhoon approaching to RLNB. Therefore swells in shallow seas could be well simulated by such higher frequency microseisms with a linear scaled correlation with observed wave heights. Findings also indicate that higher frequency of microseisms may generate near coasts compared to the source of typhoon generating microseisms at the frequency band of 0.1 and 0.2 Hz over the deep seas. Source characteristics in deep and shallow seas have been recognized by using the spectral ratio method. Since seismic levels have been well separated, the simulated extreme waves from >0.2 Hz of higher frequency microseisms have no more contaminated by the source of typhoon generating microseisms in 0.1-0.2 Hz band.

The similar pattern of spectral ratio is also found at RLNB with three different typhoons shown in Figure 4 and 5. Figure 4 shows in particular the inconsistency between microseism characteristics and observed waves during Typhoon Linfa of 2009. With the category 2 cyclone in that period, the simulated waves are much lower than the observation of 11.7 m wave height. The maximum wave of 7.5m was only observed by other buoys nearby in the same duration and wind speeds could reach to

about 20-25 m/s in this area. Despite the period of Typhoon Linfa, most of waves can be simulated by higher frequency microseisms.

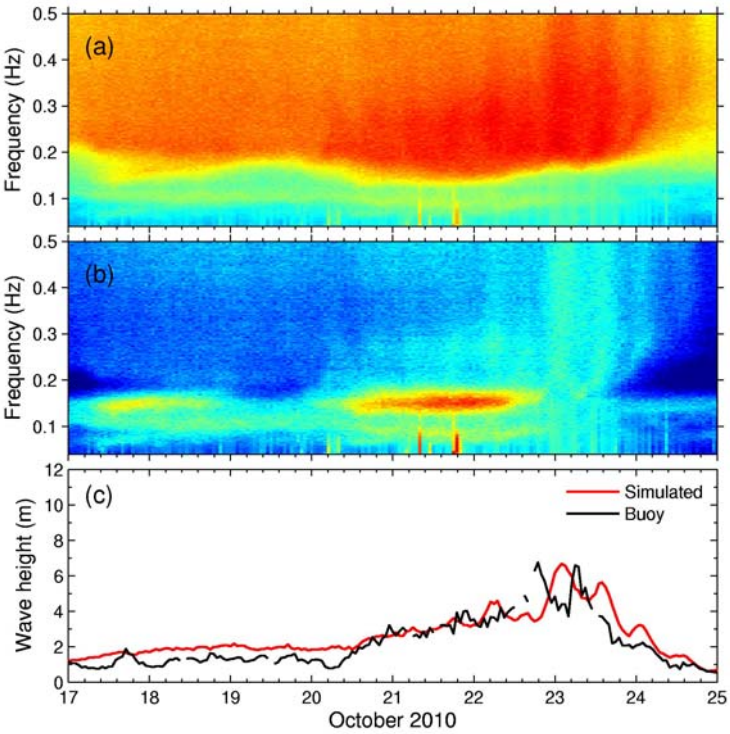

Figure 3. (a) Typhoon induced microsiesm variations in the 0.05-0.5 Hz band at RLNB. (b) The spectral ratio showing that background activities are removed by average spectrum of 10 calm days of 2010. Colors in red and blue represent the high and low energy, respectively. (c) Amplitudes of the frequency band >0.2 Hz is simulated by linear correlations (red curve) with waves observed by Cigu buoy (black curve).

Although CWB claimed that there was another wave height of 11 m observed by an experimental buoy in the same area, wind speed observations in that seas have no reason to explain the generation of such high waves. Similar comparisons were made by WAVEWATCH III model (Tolman 1991; 2009), the modeled wave heights reached to 6 m approximately and still lower than the observations at the Cigu buoy. However, the freak wave of high-order nonlinearities is not considered in this case. Simulated waves only can be produced by the wave-wave interaction generated secondary microseisms.

Figure 5 shows well simulations with the observed waves during Typhoon Talim of 2012. But the time delay between both is more than a half day. This feature could be explained by the efficiency of wave reflection coefficient (Ardhuin et al. 2011). Therefore, the swell reflection from the shoreline should be carefully examined with directional spectrum measured by buoys. Yet buoy observations at Cigu lose its direction information and similar events are required to further study the wave reflections and seismic attenuations.

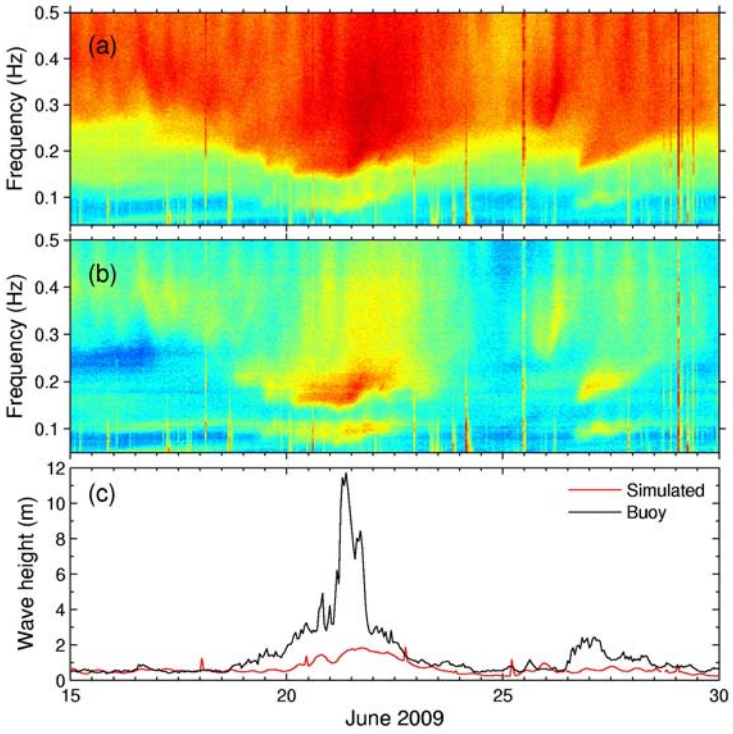

Figure 4. Same as Figure 3 but for Linfa typhoon.

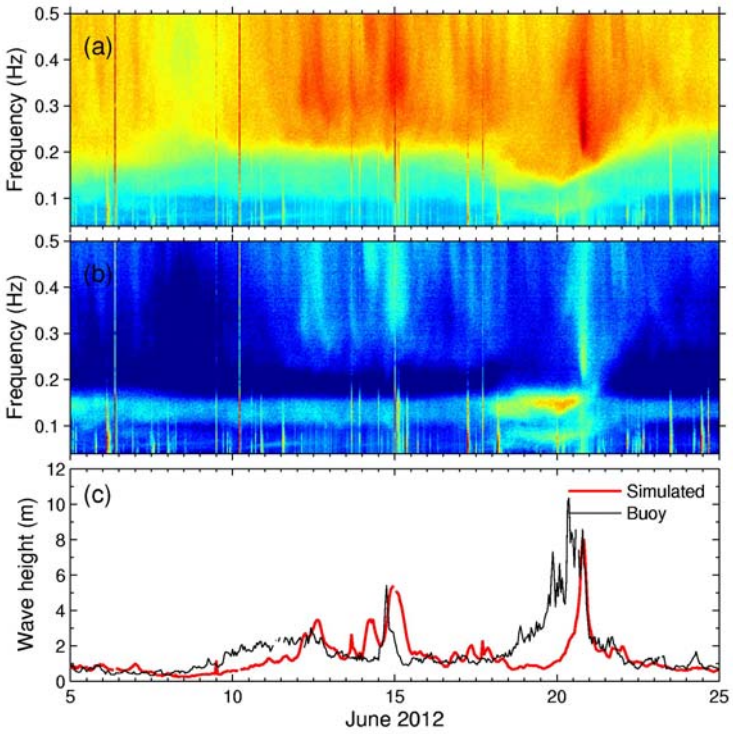

Figure 5. Same as Figure 3 but for Talim typhoon.

2. SEISMIC NOISE AT THE FREQUENCY BAND ABOVE 1 Hz

In this study we examined the source characteristic of typhoon induced secondary microseisms in the remote and shallow waters near south-western costs. In the same duration, the seismic level at frequency above 1Hz has the similar response with such high wave condition. Although shoreline

changes indeed correlate with extreme waves during typhoons, the relationship between seismic noise at such high frequency and shoreline changes or sediment transports are not clear. Yet such seismic noise could be attributed to several origins inland. One possible origin would be due to the sediment transport in rivers with high discharge levels, especially for bedload particles (Schmandt et al. 2013).

However, our seismic observations at the high frequency band have contaminated by earthquakes during three severe typhoons. Contamination may also result from the river system in the Cigu cost. Seismic observations in the monsoon season of 2011 are selected to avoid the contamination from river sediment transport. In order to investigate the seismic features in various frequencies, the frequency analysis is performed to better understand the specific spectral signature.

Figure 6 shows that dominant seismic frequency of 1-10 Hz band varies with the daily cycle starting at UTC 8:00. After the 12 hours, seismic levels then reduce to the minimum value and increases again until the next morning. The daily cycle could be due to the sea breeze circulation.

Since the flux of sediment transport is not directly measured, we may follow the assumption as the river discharge is the major force to transport the sediment, generating the likely source of seismic noise at high frequency (>1Hz). We apply the same assumption to correlate the high frequency (>1Hz) of seismic noise with waves observed in the very shallow depth as wave activity in swash zone play an important role on sediment transport.

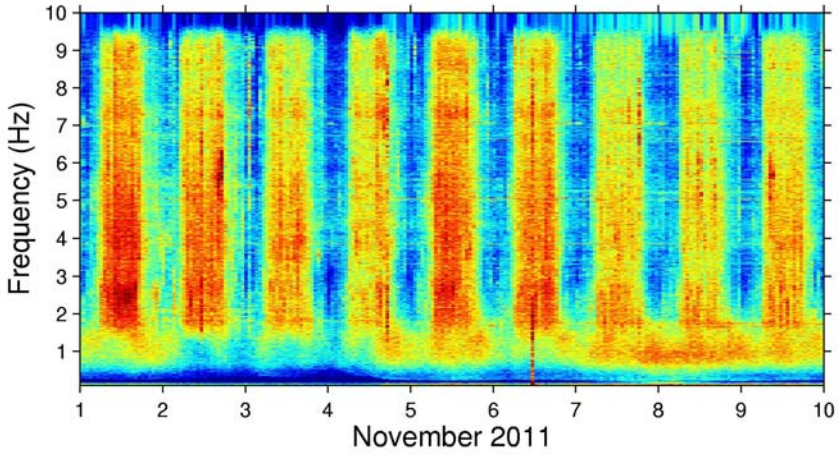

Figure 6. Spectrogram of vertical velocity in the 1-10 Hz band during the winter monsoon at RLNB seismic site.

Figure 7 shows that the high frequency (>1 Hz) variation of seismic noise follows primarily the variation in waves measured in the 4 m depth. Variations between both however are not in the same scale. In this case, waves increase up to 1m has no significant impact on seismic noise, implying that dominant frequency band should be separated to identify the correlation with waves in the swash zone. Since the energy variation is not uniformly distributed over 1-10 Hz band, the frequency band of seismic noise may result from the various origins.

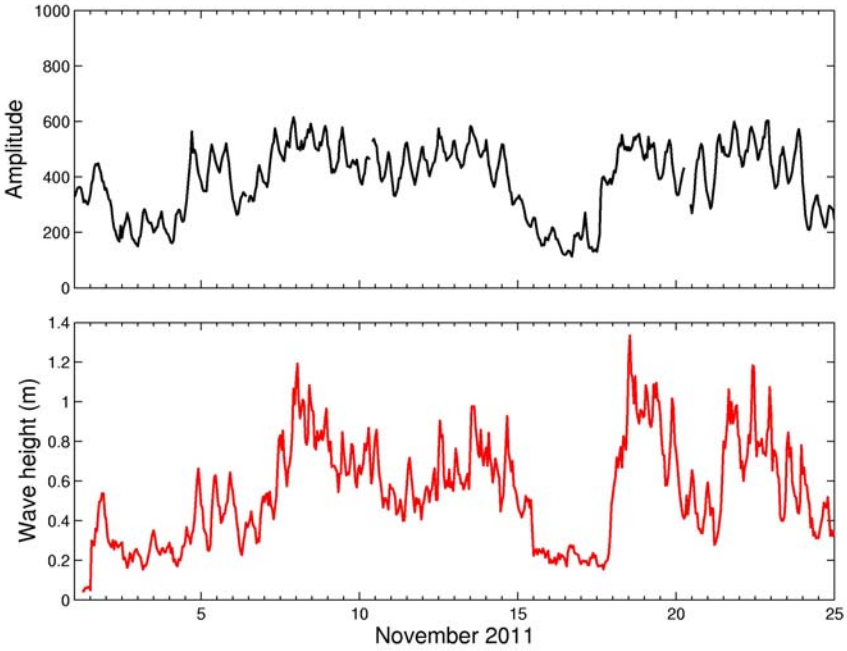

Figure7. Hourly average amplitudes (frequency band >1 Hz) recorded (upper) at RLNB with wave heights (bottom) measured at the 4 m water depth near the Cigu shoreline.

SUMMARY

In this study, the continuous seismic signals allow to investigate source characteristics in the deep and shallow seas. By the spectral ratio method, the dominant source of 0.1-0.2 Hz band is due to the wave-wave interaction in the typhoon radius. Another source of frequency band of 0.2-1 Hz results from the swell reflection from the shoreline. Results indicate that secondary microseisms observed at inland sites can be a potential tool of tracking typhoon motions and monitoring extreme waves near coasts in real time. Seismic noise in the 1-10Hz band has rough correlation with wave activities in swash zone. As the energy variation is not uniformly distributed in the whole frequency band (1-10 Hz), the detail examination should be proceeding to investigate those differences.

ACKNOWLEDGMENTS

Special thanks are due to Central Weather Bureau and Water Resource Agency, Taiwan for providing the wave data. This work was supported in part by NSC grant 103-2911-I-006-302 to National Cheng Kung University.

REFERENCES

Ardhuin, F., E. Stutzmann, M. Schimmel, and A. Mangeney. 2011. Ocean wave sources of seismic noise, *Journal of Geophysical Research*, 116, C09004.

Bromirski, P.D., F.K. Duennebi , and R.A. Stephen. 2005. Mid-ocean microseisms, *Geochemistry, Geophysics, Geosystems,* 6, Q04009.

Cooper, R.I.B., and M.S. Longuet-Higgins. 1951. An experimental study of the pressure variations in standing water waves, *Proceedings of the Royal Society of London Series A*, 206, 426–435.

Ebeling, C.W. 2012. Inferring ocean storm characteristics from ambient seismic noise, *Advances in Geophysics*, 53, 133.

Hasselmann, K. 1963. A statistical analysis of the generation of microseisms, *Reviews of Geophysics*, 1,177–210.

Haubrich, R.A., and K. McCamy. 1969. Microseisms: Coastal and pelagic sources, *Reviews of Geophysics*, 7, 539–571.

Haubrich, R., W. Munk, and F. Snodgrass. 1963. Comparative spectra of microseisms and swell, *Bulletin of the Seismological Society of America*, 53, 1032- 1039.

Hsu, L., N.J. Finnegan, and E.E. Brodsky. 2011. A seismic signature of river bedload transport during storm events, *Geophysical Research Letters*, 38, L13407.

Kao, H., and P.R. Jian. 2001. Seismogenic patterns in the Taiwan region: Insights from source parameter inversion of BATS data, *Tectonophysics*, 333, 179-198.

Kedar, S., M. Longuet-Higgins, F. W. N. Graham, R. Clayton, and C. Jones. 2008. The origin of deep ocean microseisms in the North Atlantic Ocean, *Philosophical Transactions of the Royal Society of London Series A*, 464, 1–35

Longuet-Higgins, M. 1950. A theory of the origin of microseisms, *Philosophical Transactions of the Royal Society of London Series A*, 243, 2–36.

Rabinovich, A.B. 1997. Spectral analysis of tsunami waves: Separation of source and topography effects, *Journal of Geophysical Research*, 102, 12,663–12,676.

Schmandt,B., R.C. Aster, D. Scherler, V.C. Tsai, and K. Karlstrom. 2013. Multiple fluvial processes detected by riverside seismic and infrasound monitoring of a controlled flood in the Grand Canyon. *Geophysical Research Letters*, 40, 4858–4863

Stephen, R.A., F.N. Spiess, J.A. Collins, J.A. Hildebrand, J.A. Orcutt, K.R. Peal, F.L.Vernon, and F.B. Wooding. 2003. Ocean Seismic Network Pilot Experiment, *Geochemistry*, *Geophysics*, *Geosystems*, 4, 1092.

Tabulevich, V.N., G.V. Anikanova, and E.N. Chernykh. 1976. Power, energy and position determination for excitation sources of microseisms in the North Atlantic Ocean from the international data 16018 March, 1968, *Acta Universitatis Ouluensis, Series A, Scientiae Rerum Naturalium*, 43, 83–90.

Tolman, H.L. 1991. A third generation model for wind on slowly varying, unsteady and inhomogeneous depth and currents, *Journal of Physical Oceanography*, 21, 766–781.

Tolman, H.L. 2009. *User manual and system documentation of WAVEWATCH-III™ version 3.14*, Tech. Rep. 276, National Oceanic and Atmospheric Administration, Camp Springs, Md.

Vich, M., and S. Monserrat. 2009. Source spectrum for the Algerian tsunami of 21 May 2003 estimated from coastal tide gauge data, *Geophysical Research Letters*, 36, L20610.

Wiechert, E. 1904. Discussion, verhandlung der zweiten Internationalen Seismologischen Konferenz, *Beitrage zur Geophysik*, 2, 41–43.